Scintillation Response of Liquid Xenon
to Low Energy Nuclear Recoils

E. Aprile,* K. L. Giboni, P. Majewski, K. Ni, and M. Yamashita

Physics Department and Astrophysics Laboratory,

Columbia University, New York, NY 10027

R. Hasty, A. Manzur, and D. N. McKinsey

Department of Physics, Yale University,

P.O. Box 208120, New Haven, CT 06520

(Dated: February 2, 2008)

Abstract

Liquid Xenon (LXe) is expected to be an excellent target and detector medium to search for dark matter in the form of Weakly Interacting Massive Particles (WIMPs). Knowledge of LXe ionization and scintillation response to low energy nuclear recoils expected from the scattering of WIMPs by Xe nuclei is important for determining the sensitivity of LXe direct detection experiments. Here we report on new measurements of the scintillation yield of Xe recoils with kinetic energy as low as 10 keV. The dependence of the scintillation yield on applied electric field was also measured in the range of 0 to 4 kV/cm. Results are in good agreement with recent theoretical predictions that take into account the effect of biexcitonic collisions in addition to the nuclear quenching effect.

PACS numbers: 14.60.Pq, 26.65.+t, 29.40.Mc, 95.35.+d

---
*Electronic address: age@astro.columbia.edu

I. INTRODUCTION

Astrophysical observations strongly support the view of a Universe in which about 23% of the matter is non-luminous and non-baryonic[1]. A leading candidate for this non-baryonic matter is the Weakly Interacting Massive Particle (WIMP). WIMPs are cold thermal relics of the Big Bang, moving non-relativistically at the time of structure formation. If they exist, these particles can be detected via their elastic collisions with nuclei of ordinary matter. The typical energy of the resulting nuclear recoils is a few tens of keV and the predicted interaction rate is in the range 0.1 - 0.0001 $kg^{-1}day^{-1}$[2, 3]. Experiments so far have achieved sensitivities down to approximately 0.1 $kg^{-1}day^{-1}$ without a positive detection[4], with the exception of the DAMA experiment, which has reported a significant annual modulation signal attributed to dark matter events[5]. Intense efforts are underway worldwide to realize more sensitive experiments, with increased target mass and improved background rejection capabilities.

Among the suggested target materials for direct detection of WIMPs, liquid xenon (LXe) is promising because of its relatively large cross-section for spin-independent WIMP-nucleon scattering and its excellent ionization and scintillation properties. Effective and redundant background rejection schemes with a target mass in the 1000 kg range are perhaps the most attractive features of a LXe-based experiment for dark matter, with the additional advantage of being sensitive also to purely spin-dependent WIMP-nucleon interactions. Independent experimental programs using LXe in a variety of detector concepts are currently being pursued in Europe, Japan and the USA [6, 7, 8, 9, 10, 11]. All these concepts make use of the excellent scintillation properties of LXe, which has the highest light yield among noble liquids, comparable with the best crystal scintillators.

The scintillation light yield produced by a nuclear recoil in LXe is quite different from that produced by an electron recoil of the same energy. The ratio of these two yields, when no electric field is applied, has been previously measured[12, 13, 14, 15], but the data do not cover the lowest recoil energies, which are of interest to sensitive dark matter experiments. Here we report results obtained with a LXe detector exposed to a neutron beam to measure Xe recoil scintillation efficiency in the energy range from 10.4 keV to 56.5 keV. Since some of the LXe dark matter experiments operate with an external electric field to simultaneously detect the scintillation and ionization signals produced by nuclear recoils, we have also

measured the scintillation yield as a function of applied electric field up to 4 kV/cm. In the first part of the paper, the experimental apparatus and method is described. Following a presentation of the data, the experimental results are discussed in terms of recent theoretical predictions.

II. EXPERIMENTAL APPARATUS

A. Liquid Xenon Detector

The LXe detector used for these measurements is shown schematically in Figure 1. It is the same detector that was recently used to investigate the anticorrelation of ionization and scintillation of LXe and the improvement in gamma-ray energy resolution[16]. Details on the detector's electrodes, light sensors, gas purification with continuous circulation, and cryogenic system have been reported elsewhere[17, 18]. We recall the main features relevant for the measurements reported in this paper. The active volume of 7.1 cm^3 is defined by a cylinder made of polytetrafluoroethylene (PTFE), on which two photomultiplier tubes (PMTs) are mounted. The compact PMTs are Hamamatsu R9288, with response optimized for Xe light (175 nm). They have been shown to work reliably at LXe temperature and to withstand pressure up to 5 bar. The two PMTs view the active liquid through a set of wire meshes used as the cathode, shielding grid and anode of an ionization chamber. The meshes have 95% optical transmission. The fourth mesh, in front of the PMT facing the cathode, is used to minimize cross-talk between light and charge signals when detected simultaneously. PTFE material is used as a reflector for the Xe light [19]. To study the electric field dependence of the scintillation produced by electron and nuclear recoils, a uniform electric field is created with appropriate potentials on the meshes. In independent measurements with the same detector, before and after neutron irradiation, we used its capability as a time projection chamber, triggered by the scintillation light, to establish the purity level of the liquid and its stability with time. For gain calibration of the PMTs, a blue LED was mounted on the PTFE cylinder.

The assembled PTFE structure with meshes and PMTs is closed in a stainless steel vessel that is supported from the top flange and sealed with a Cu gasket. Ports for pumping and gas filling, as well as multiple hermetic feedthroughs for high voltage and signal connections,

3

are also mounted on the top flange. The detector vessel is enclosed by a vacuum cryostat and cooled with liquid nitrogen as described in [20]. To completely cover the assembled PTFE and PMT structure with LXe, a total of 3.8 kg of Xe gas was condensed in the vessel after passage through a high temperature metal getter to remove impurities. The temperature of the liquid was maintained at 178 ± 1 K by controlling the vapor pressure. For calibration of the detector with gamma-rays, radioactive sources of [57]Co and [22]Na were used, mounted below the vacuum cryostat. For measurements of the light and charge yields of alpha particles in the same detector, we used an internal [241]Am source deposited on the center of the cathode.
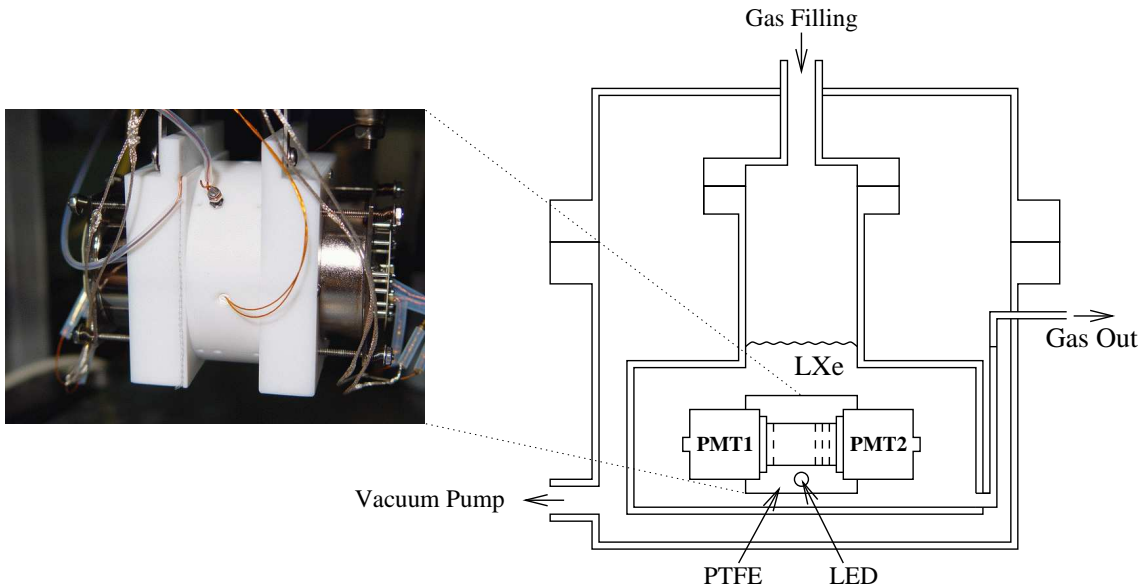

FIG. 1: Schematic view and photograph of the LXe detector assembly. The vacuum cryostat surrounding the detector vessel and the cooling system are not shown.

B. Neutron Beam Setup

The experiments were carried out in the Radiological Research Accelerator Facility at the Columbia Nevis Laboratory. The neutrons were produced by bombarding a tritiated target with 3.3 MeV protons. A nearly mono-energetic neutron beam with an average energy of 2.4 MeV in the forward direction was obtained through the $T(p, n)^3He$ reaction. The energy spread of the neutrons due to the finite thickness of the tritium target is less than 10% FWHM. The liquid xenon detector was placed 60 cm from the neutron source in the

4

forward direction.

The energy of a xenon recoil can be determined simply from kinematics. The recoil energy E_r transferred to a xenon nucleus when a neutron with energy E_n scatters through an angle θ is approximately

$$E_r \approx E_n \frac{2M_n M_{Xe}}{(M_n + M_{Xe})^2}(1 - \cos\theta), \tag{1}$$

where M_n is the mass of a neutron and M_{Xe} is the mass of a xenon nucleus. The energy transferred is maximum for back-scattered neutrons. A BC501A liquid scintillator (7.5 cm diameter, 7.5 cm long) with pulse shape discrimination was used to tag the neutrons scattered in the LXe detector.

The position and size of the neutron detector determine the average and spread of the xenon recoil energy of the tagged events. Data were taken with the center of the BC501A detector at neutron scattering angles of 123, 117, 106, 72, 55 and 44 degrees. The distance between the BC501A and LXe detectors was near 50 cm for all angles. To minimize the chance of direct neutron scattering in the liquid scintillator, the path between the neutron source and the neutron detector was shielded with 30-cm-thick borated polyethylene (5% by weight natural boron). The energy spread due to the finite solid angle of the BC501A neutron detector was approximately 10% FWHM.

C.   Data Acquisition

The data acquisition was done with a digital sampling oscilloscope (LeCroy LT374), triggered by NIM coincidence logic. A block diagram of the electronics and data acquisition system is shown in Figure 2. The analog signals from the LXe PMTs and the BC501A PMT were split, with one copy going to a discriminator for each channel. The amplification and discrimination on the LXe channels was set to achieve a single photoelectron threshold. A coincidence unit was used to trigger the oscilloscope on triple coincidences among the two LXe PMTs and the BC501A PMT within 150 ns.

The recorded waveforms were transferred to a PC for later analysis. All waveforms were sampled at 1 GHz for 500 ns. For the LXe waveforms, the gain on the oscilloscope input was adjusted to an appropriate value for each scattering angle. The signal from the BC501A detector was digitized at two different gains to extend the dynamic range. Event timing and signal integrals were determined in software for the data analysis.
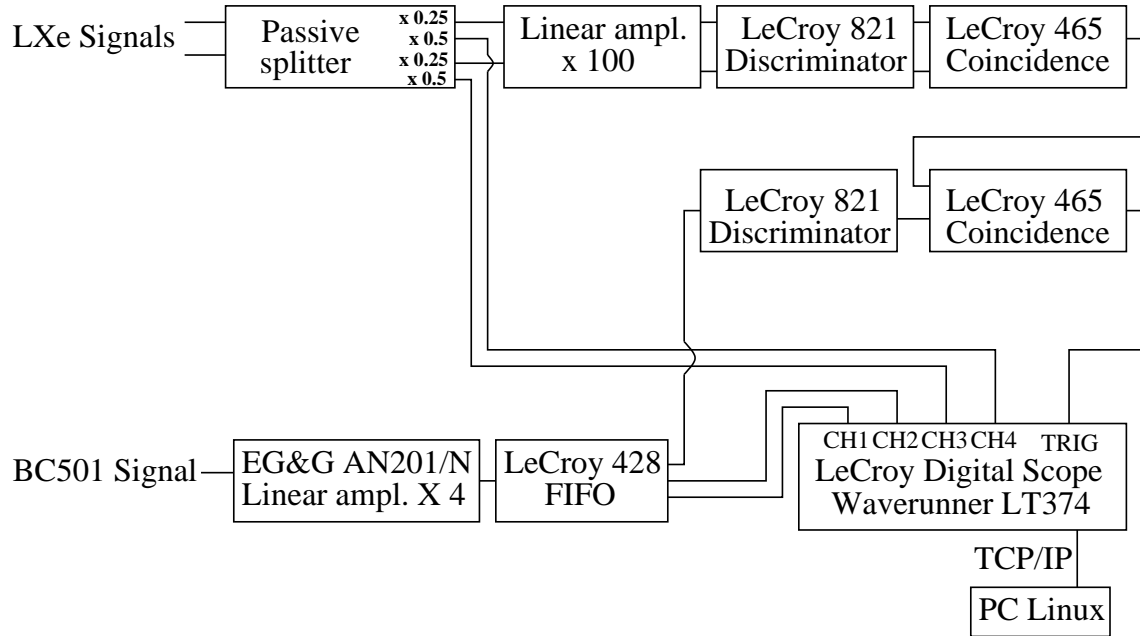
FIG. 2: Schematic of data acquisition system

III.   DATA ANALYSIS AND RESULTS

A.   LXe Scintillation Efficiency as a Function of Recoil Energy

The scintillation efficiency for Xe nuclear recoils is defined as the ratio of the light produced by a nuclear recoil to the light produced by an electron recoil of the same energy. In practice, the peak in the nuclear recoil spectrum measured at each scattering angle is converted to an electron equivalent energy scale and compared to the expected nuclear recoil energy at that angle. The electron equivalent scale is determined by calibrating the LXe detector with 122 keV gamma rays from ^{57}Co, and the expectation value of the nuclear recoil energy is calculated from the geometry of the LXe and BC501A detectors, as in Equation 1.

For the calibrations, a ^{57}Co source was placed directly underneath the cryostat, and the oscilloscope was triggered on the coincidence between the two LXe PMTs. The resulting scintillation light spectrum at zero electric field is shown in Figure 3. When the 122 keV peak location in the light spectrum is combined with the gain measurement from the single photon peak, the sensitivity is found to be 6 photoelectrons/keV. The measured sensitivity and spectrum are in good agreement with a simulation of the detector response, which takes into account the light collection efficiency and its spatial distribution as described in [17].
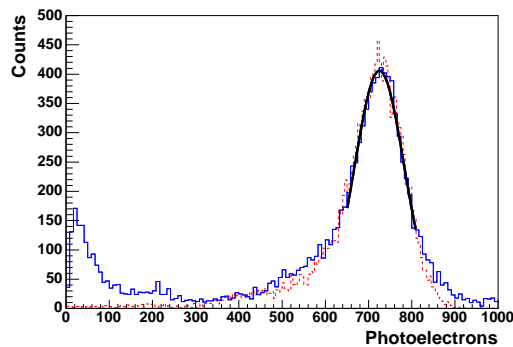
6

FIG. 3: ^{57}Co scintillation light spectrum at zero field (solid line). A fit to the 122 keV peak gives a light yield of about 6 photoelectrons/keV, which is very close to the expected value from simulation (dashed line).

The selection of nuclear recoil events is based primarily on time of flight between the LXe and the BC501A detectors. For elastic scattering events where the neutron scatters directly from a Xe nucleus to the BC501A detector, the time of flight is approximately 2 ns for every centimeter of separation. Neutron and gamma coincidences are well separated in the time of flight (ToF) spectrum, as can be seen in Figure 4a. Because of the finite size of the detectors, the ToF for neutrons that only scatter once in the active LXe varies by 6 ns. Neutron events in which multiple scattering occurs will generally have a longer ToF than single scattering events, and they also contribute to a tail on the neutron peak in the ToF spectrum. Only events within the first 6 ns of the neutron peak are accepted.

The single event rate in both the LXe and BC501A detectors is high enough that the accidental coincidence rate is approximately equal to the tagged neutron event rate. Pulse shape discrimination (PSD) and energy deposition in the BC501A are used to eliminate some of the accidental coincidences. The PSD is based on the ratio of excited states with different lifetimes in the BC501A[21]. The ratio of long and short lived excited states is different for gamma and neutron events in the BC501A. A 2 MeV energy cut in the BC501A eliminates neutrons with too low an energy to have come from single scattering events in xenon. With PSD and BC501A energy deposition cuts, the accidental rate is reduced by approximately a factor of four. The ToF distribution after these cuts is shown in Figure 4b. Note that the energy cut is in units of keV electron equivalent, keV$_{ee}$.

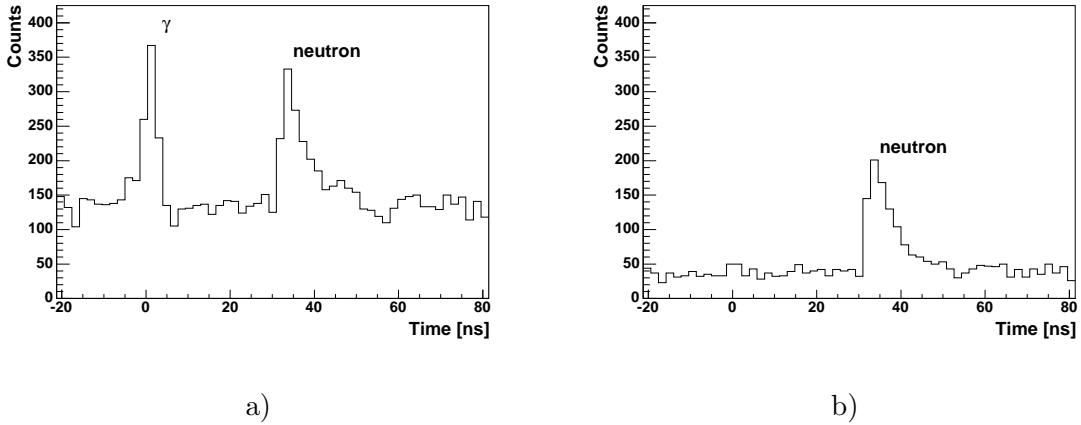The accidental spectrum has a negligible effect on the location of the nuclear recoil

FIG. 4: Time of flight distributions recorded using the LXe and BC501 detectors. a) includes events that passed either the neutron or the gamma PSD cut and deposited less than 20 keV$_{ee}$ in the LXe. b) includes events that passed the neutron PSD cut and deposited less than 20 keV$_{ee}$ in the LXe.

peak in the LXe energy deposition spectrum for all but the 10 keV nuclear recoil data. In order to reduce the effect of the accidental background on this energy spectrum, an accidental spectrum is formed from events with a ToF far from both the gamma and neutron ToF peaks. The electron equivalent energy deposition in the LXe of the vast majority of accidental coincidences is above the energy range of interest in these measurements, however a significant number of accidental events have LXe energy depositions below 1 keV electron equivalent energy. The relatively high cross section for small scattering angle neutron scattering could explain the higher rate of low energy accidental events in the 10 keV nuclear recoil data.

The electron equivalent energy spectra for nuclear recoil events with the lowest (10.4 keV) and highest (56.5 keV) recoil energies are shown in Figure 5, together with the accidental spectrum. The peaks are fit with the sum of a Gaussian and an exponential distribution. The peak location of the Gaussian is divided by the expected recoil energy to determine the scintillation efficiency. The resulting relative scintillation efficiency, as a function of nuclear recoil energy, is shown in Table III A. For recoil energies below 40 keV, where no prior measurements have been reported, the scintillation efficiency drops to 0.13. The errors include both statistical and systematic uncertainties, of similar sizes. The dominant systematic uncertainties are due to the uncertainty in the position of the detectors and the

8

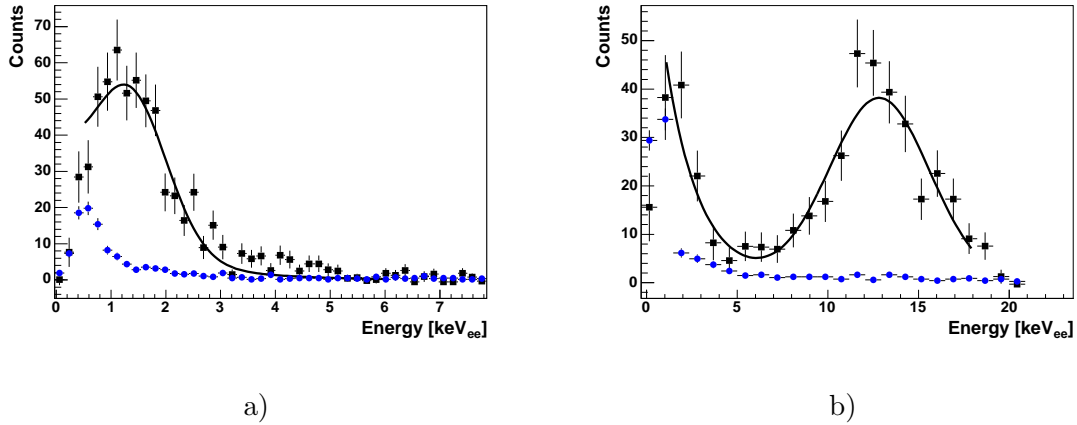a)   b)

FIG. 5: The measured LXe scintillation spectra (filled squares) for the (a) 10.4 keV and (b) 56.5 keV nuclear recoil data. The accidental spectrum is shown with filled circles. In both cases the uncertainties are statistical.

effects of multiple scattering. This last contribution has been evaluated with Monte Carlo simulations as discussed in Section III C.

θ (degrees)	E_r (keV)	Relative Efficiency
44	10.4	0.130 ± 0.024
55	15.6	0.163 ± 0.023
72	25.6	0.167 ± 0.021
106	46.8	0.238 ± 0.030
117	53.2	0.240 ± 0.019
123	56.5	0.227 ± 0.016

TABLE I: The relative scintillation efficiency of Xe nuclear recoils relative to that of gamma rays of the same energy.The average scattering angle of the neutrons is given by θ. The average recoil energy of the xenon nucleus is given by E_r. Uncertainties include both systematic and statistical contributions.

9

B. LXe scintillation efficiency as a function of electric field

The dependence of the LXe scintillation efficiency on the applied electric field was investigated for a recoil energy of 56.5 keV. With scattering angle fixed, measurements were carried out at different electric fields across the LXe detector, up to 4 kV/cm. The scintillation efficiency for the 56.5 keV recoils at a given field is calculated relative to the scintillation efficiency at zero field, which eliminates uncertainties associated with the determination of the recoil energy. The gain of the PMTs in LXe under prolonged neutron irradiation was observed to change by approximately 10%. The data have been corrected for this gain change and are shown in Figure 6. The error bars include the systematic error due to the variation in PMT gain. Due to limited beam availability and having verified that the scintillation yield above 1 kV/cm was not changing appreciably, we decided to concentrate the measurements at fields below 1 kV/cm. In the same figure we have also plotted the scintillation yield measured with the same detector under 5.5 MeV alpha irradiation and under 122 keV gamma-ray irradiation. The ionization yield for alpha particles is shown as well. As previously measured in LXe[22, 23], the strong recombination rate along alpha particle tracks is such that only about 6% of the liberated charges are collected even at 5 kV/cm, whereas more than 90% are collected for 1 MeV electrons at the same field. The measurements with the weak alpha particle or gamma-ray sources were carried out prior to exposing the LXe detector to the neutron beam.

C. Monte Carlo simulation

The effect of multiple scattering of neutrons in the LXe detector and surrounding materials on the location of the nuclear recoil peak was investigated with a Monte Carlo simulation. A comparison of the simulated recoil spectra including multiple scattering events with the spectra generated with only single scattering events is used to estimate the significance of multiple scattering. The simulations were carried out using the GEANT4 LHEP-PRECO-HP physics package[24].

All the geometries used for the five energies reported in this paper are simulated. The simulations include the LXe detector and its surrounding cryostat, the shielding materials, and the neutron detector. Neutrons with an energy of 2.4 MeV are generated from the
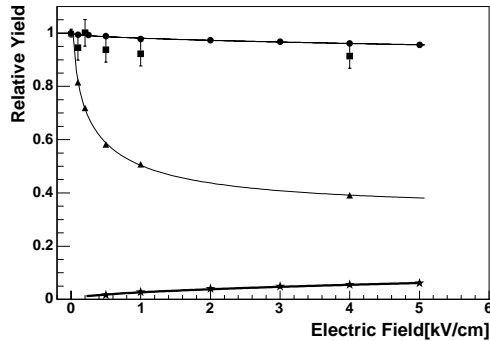
FIG. 6: The LXe scintillation efficiency (squares) for 56.5 keV nuclear recoils, as a function of applied electric field, relative to the zero field efficiency. The uncertainty on the zero field data point is the statistical uncertainty on the location of the peak in the nuclear recoil spectrum, while the uncertainty on the data points with an applied field is dominated by the uncertainty in the gain of the photomultipliers. For comparison, we also show scintillation data obtained with the same detector for 5.5 MeV alpha particles (circles) and for 122 keV gamma-rays (triangles). We also show ionization data for alpha particles (stars).

location of the neutron source with velocities distributed uniformly over a cone large enough to cover the LXe detector.

For events in which energy is deposited in both the LXe and BC501A detectors, the timing, energy deposition and type of each interaction is recorded and used to calculate the simulated spectra. The ToF information is used to reduce the effects of the multiple scattering. As in the experimental data, spectra are constructed from events with a ToF between the two detectors that is compatible with single scattering. The simulated spectra are also broadened with the detector resolution.

The multiple scattering has little effect on the location of the peak found by fitting the nuclear recoil spectrum, as shown in Figure III C a) and b) where the results for single scattering are drawn in a scaled histogram. For each geometry, the single scattering spectrum is fit with a Gaussian distribution to determine the peak location; the multiple scattering spectrum is fit with a Gaussian and an exponential distribution. The difference in the peak location is less than five percent for every geometry. Simulated spectra for the lowest and highest energy deposition geometries are shown in Figure III C. It is interesting to note that the expected decreasing efficiency for low energy nuclear recoils has the effect of further
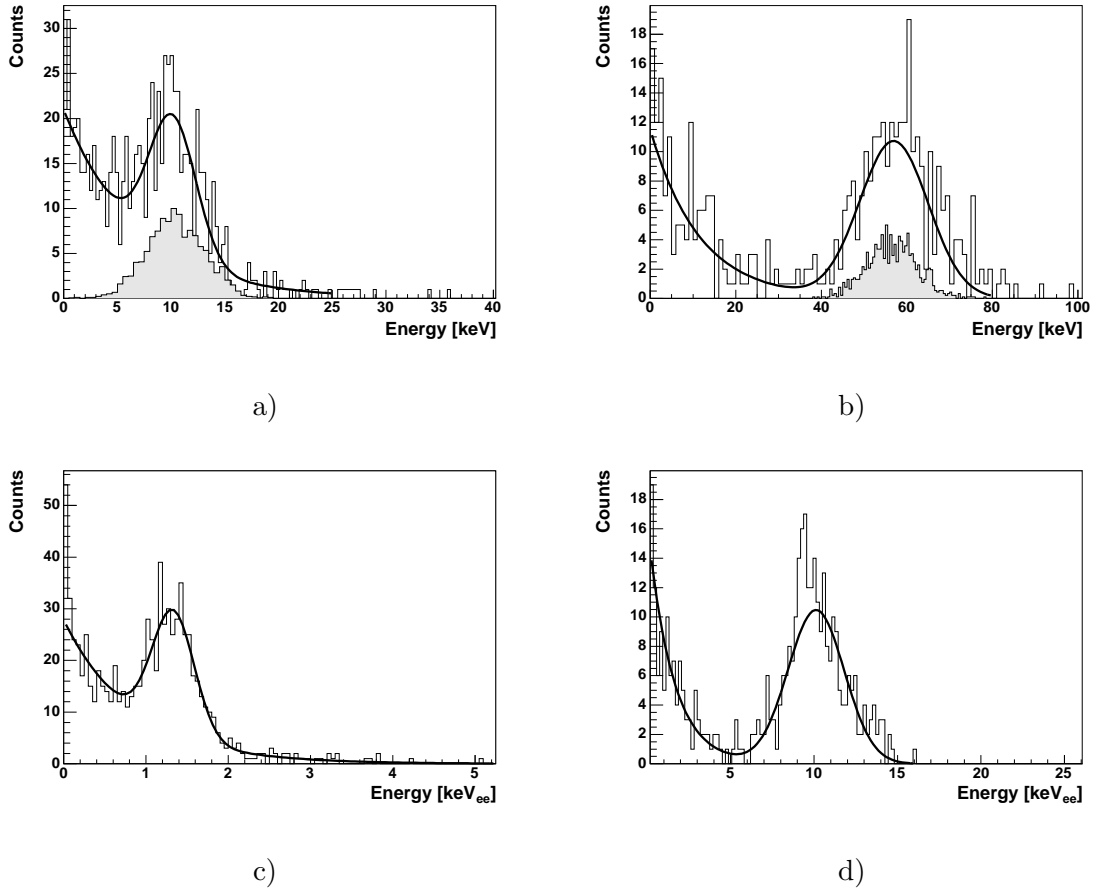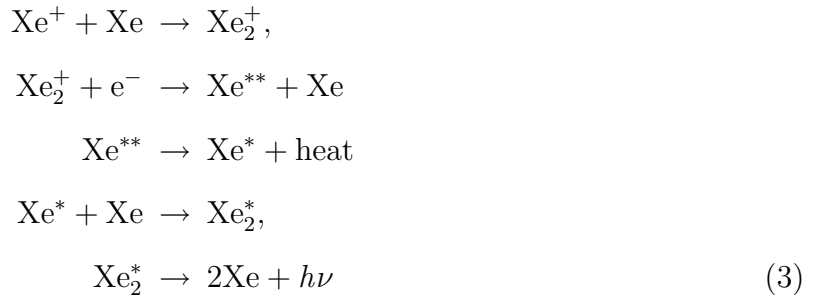
FIG. 7: Monte Carlo simulations of neutron scattering in the LXe detector. a) Histogram of energy deposition, with $\theta = 44°$ (average energy deposition of 10.4 keV for single elastic scattering events); b) Histogram of energy deposition, with $\theta = 123°$ (average energy deposition of 56.5 keV for single elastic scattering events); c) and d) are the same as a) and b), with the energy of each single elastic scattering event multiplied by the theoretically predicted scintillation efficiency[26]. The shaded histogram represents the single scattering results.

reducing the electron equivalent energy for low energy multiple scattering events.

IV. INTERPRETATION AND SUMMARY OF RESULTS

We have measured the scintillation efficiency of nuclear recoils in LXe relative to that of 122 keV gamma rays from ^{57}Co. For recoils with energy in the range of 10.4 to 56.5 keV, we find the relative scintillation efficiency to be in the range 0.13 to 0.23. For the lowest recoil energies, our data are the first reported, to our knowledge. Compared to the scintillation

yield due to electron or alpha particle excitation, the scintillation yield due to nuclear recoil excitation is significantly reduced. Our results are shown in Figure 8, along with previous measurements by other groups[12, 13, 14, 15]. The predicted curves from theoretical models from Lindhard [25] and Hitachi[26] are also shown as solid and dotted lines, respectively. The scintillation efficiency of LXe is about 15% less than the Lindhard prediction. Hitachi explains this difference by estimating the additional loss in scintillation yield that results from the higher excitation density of nuclear recoils. The origin of the VUV scintillation light is attributed to two separate processes[27]:

$$Xe^* + Xe \rightarrow Xe_2^*,$$
$$Xe_2^* \rightarrow 2Xe + h\nu \tag{2}$$

$$Xe^+ + Xe \rightarrow Xe_2^+,$$
$$Xe_2^+ + e^- \rightarrow Xe^{**} + Xe$$
$$Xe^{**} \rightarrow Xe^* + heat$$
$$Xe^* + Xe \rightarrow Xe_2^*,$$
$$Xe_2^* \rightarrow 2Xe + h\nu \tag{3}$$

In these equations, Xe^* and Xe^+ are excitons and ions that are produced by the ionizing radiation, and $h\nu$ denotes the scintillation photons of 175 nm wavelength. In both Equation 2 and Equation 3, one exciton or ion produces one ultraviolet photon.

Rapid recombination in LXe under high Linear Energy Transfer (LET) excitation[28, 29] provides a mechanism for reducing the scintillation yield of nuclear recoils in addition to that of nuclear quenching treated by Lindhard. In order to estimate the total scintillation yield, Hitachi considers biexcitonic collisions, or collisions between two "free" excitons that emit an electron with a kinetic energy close to the difference between twice the excitation energy E_{ex} and the band-gap energy E_g (i.e. $2E_{ex}$ -E_g):

$$Xe^* + Xe^* \rightarrow Xe + Xe^+ + e^- \tag{4}$$

The electron then loses its kinetic energy very rapidly before recombination. This process reduces the number of excitons available for VUV photons since it requires two excitons to eventually produce one photon. It is therefore considered the main mechanism responsible
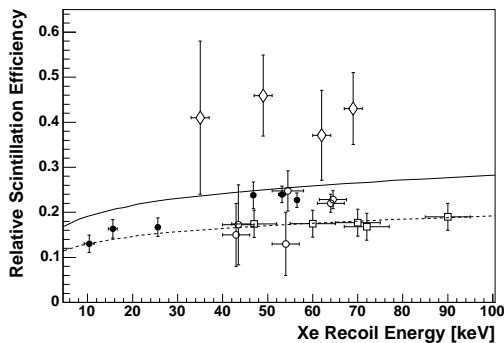
FIG. 8: The relative scintillation efficiency for nuclear recoils as a function of the Xe recoil energy in LXe. The full circles are the data from this experiment. The uncertainties include both statistical and systematic uncertainties. Also shown are measurements by other groups: open circles, squares, and diamonds show the data from Akimov *et al.*[12], Arneodo *et al.*[14], and Bernabei *et al.*[13] respectively. The solid line is from Lindhard[25] and the dotted line is from Hitachi's[26] theoretical model.

for the reduction of the total scintillation yield in LXe under irradiation by nuclear recoils. As shown in Figure 8, our data are in good agreement with the Hitachi prediction.

The simultaneous measurement of the scintillation and the ionization of nuclear and electron recoils in a LXe dark matter detector can be a powerful tool for background rejection. As shown in Figure 6, the electric field dependence of the scintillation yield of a Xe recoil is not very different than that already known for alpha particles in LXe. Even at the highest field of 4 kV/cm, recombination is very strong and the light yield is suppressed by less than 5 %. The field dependence of the scintillation and the charge yields are related [31],

$$\frac{S(E)}{S_0} = (1 - \frac{Q(E)}{Q_\infty} + N_{ex}/N_i - \chi)/(1 + N_{ex}/N_i), \qquad (5)$$

where S_0 (Q_∞) and $S(E)$ ($Q(E)$) are the number of photons (charges) at zero (infinite) electric field and electric field E. N_{ex} and N_i are the number of excitations and ion pairs produced by the ionizing radiation, and χ is the fraction of escaping electrons at zero electric field. In this case, the escape electron fraction is negligible ($\chi = 0$).

The ionization yield $Q(E)/Q_\infty$, in the presence of strong recombination such as along an alpha particle track, can be described by $Q(E)/Q_\infty = aE^b$, with E in kV/cm. The result of a fit with this empirical function to the alpha ionization data shown in Figure 6 gives a

14

= 0.021 ± 0.004 and $b = 0.52 \pm 0.14$, consistent with values obtained from fitting previous alpha ionization data in LXe [30]. Using the fitted parameters, we estimate the number of electrons collected by an external field E, for the case of a nuclear recoil of energy E_r, to be $Q(E) = (E_r q_{nc}/W) a E^b$, where $W = 15.6$ eV is the average energy required to produce an electron and ion pair[31] and q_{nc} is the nuclear quenching factor from Lindhard theory. For a 56.5 keV nuclear recoil in LXe, under a field of 5 kV/cm, we would then expect about 50 ionization electrons. A direct measurement of the charge associated with Xe nuclear recoils will be carried out in the near future using a dual phase (gas/liquid) XENON prototype.

In summary, we have measured the scintillation efficiency for Xe recoils relative to 122 keV gamma-rays using a detector equipped with PMTs immersed in the liquid for enhanced light collection. The high photoelectron yield of 6 photoelectrons/keV has allowed us to measure for the first time the scintillation efficiency of Xe recoils with energy as low as 10 keV. The scintillation response for low energy nuclear recoils is of great relevance to LXe dark matter searches designed to probe the lowest spin-independent WIMP-nucleon cross-section predictions.

V.   ACKNOWLEDGEMENTS

---

[1] D. N. Spergel *et al.*, Astrophys. J. Suppl. **148**, 175 (2003).

[2] M. W. Goodman and E. Witten, Phys. Rev. **D31** 3059 (1985).

[3] G. Jungman, M. Kamionkowski, and K. Griest, Phys. Rep. **267**, 195 (1996).

[4] CDMS collaboration, Phys. Rev. Lett. **93**, 211301 (2004).

[5] DAMA collaboration, Riv. N. Cim. **26**, 1 (2003).

[6] P. F. Smith, Phil. Trans. R. Soc. Lond. A **361**, 2591 (2003).

[7] D. B. Cline *et al.*, Nucl. Phys. B (proc. Suppl.) **124**, 229 (2002).

[8] R. Bernabei *et al.* (DAMA Collaboration), Phys Lett B **436**, 379 (1998).

[9] Y. Suzuki, hep-ph/0008296.

[10] M. Yamashita *et al.*, Astroparticle Physics **20**, 79 (2003).

[11] E. Aprile *et al.* (XENON Collaboration) astro-ph/0407575.

[12] D. Akimov *et al.*, Phys. Lett. B **524**, 245 (2002).

[13] R. Bernabei *et al.* EPJdirect **C11**, 1 (2001).

[14] F. Arneodo *et al.*, Nucl. Inst. Meth. A **449**, 147 (2000).

[15] Bernabei *et al.*, Phys Lett **B389**, 757 (1996).

[16] E. Aprile *et al.*, "Energy Resolution of Liquid Xenon from Simultaneous Measurement of Ionization and Scintillation", submitted to Nucl. Inst. and Meth. A (2005).

[17] E. Aprile *et al.*, "Scintillation Spectroscopy with Photomultipliers in Liquid Xenon", submitted to Nucl. Inst. and Meth. A (2005).

[18] K.L Giboni *et al.*, "Fast Timing Measurements of Gamma Ray Events in Liquid Xenon", submitted to IEEE Trans. Nucl. Sci. (2005).

[19] M. Yamashita, et al., Nucl. Inst. and Meth. A, **535**, 692 (2004).

[20] E. Aprile *et al.*, Nucl. Inst. and Meth. A **480**, 636 (2002).

[21] S. Marrone *et al.*, Nucl. Inst. and Meth. A **490**, 299 (2002).

[22] E. Aprile, R. Mukherjee, and M. Suzuki, IEEE Trans. Nucl. Sci **37**, 553 (1990).

[23] E. Aprile, R. Mukherjee, and M. Suzuki, Nucl. Inst. and Meth. A **302**, 177 (1991).

[24] S. Agostinelli *et al.*, Nucl. Inst. and Meth. A **506**, 250 (2003).

[25] J. Lindhard, Mat. Fys. Medd. Dan. Vid. Selsk. **33** 1 (1963).

[26] A. Hitachi, in *The Identification of Dark Matter* Proceedings of the Fourth International Workshop, York, UK 2 - 6 September 2002, edited by Neil J C Spooner and Vitaly Kudryavtsev (University of Sheffield, UK) p 357-362; 5th International Workshop on the Identification of Dark Matter, IDM2004, Edinburgh, Scotland, 6th-10th September 2004.

[27] S. Kubota *et al.*, Phys. Rev. B **17**, 2762 (1978).

[28] A. Hitachi *et al.*, Phys. Rev. B **27**, 5279 (1983).

[29] A. Hitachi, T. Doke, and A. Mozumder, Phys. Rev. B **46**, 11463 (1992).

[30] H. Ichinose *et al.*, Nucl. Inst. and Meth. A **305**, 111 (1991).

[31] T. Doke *et al.*, Jpn. J. Appl. Phys. **41**, 1538 (2002).